Dynamics of a street canyon flow from idealized field and wind tunnel experiments

Karin Blackman[1], Laurent Perret[1], Eric Savory[2]

[1]*LUNAM Université, École Centrale de Nantes, LHEEA UMR CNRS 6598, Nantes Cedex 3, France, Karin.Blackman@ec-nantes.fr, Laurent.Perret@ec-nantes.fr*

[2]*Dept of Mechanical & Materials Engineering, Faculty of Engineering, Univ of Western Ontario, London, Canada, esavory@uwo.ca*

dated : 15 June 2015

ABSTRACT

The present work examines the flow field in a simple street canyon that has been modeled at full-scale and at 1:200 scale in a wind tunnel. It relies on the detailed analysis of statistics of both flows including two-point correlation coefficients, an approach not commonly done for canyon flows. Comparison between the field and wind tunnel study has demonstrated good agreement for the mean velocity and turbulence statistics, which are typically within 20%. However, significant differences in the along-canyon mean and turbulent components have been observed and are shown to be a result of the changing of the ambient wind direction and low frequency motion present in the field. As the wind direction changes over time the result is a channeling of flow along the canyon axis. This phenomenon cannot be accurately reproduced by the wind tunnel model, which produces nominally 2D flow. The turbulence dynamics were investigated through two-point spatial correlation of the streamwise, spanwise and vertical components, which show agreement to within 15-30% between the field and wind tunnel results. Finally, it is shown how the application of a Stochastic Estimation (SE) method, using spatially well-resolved wind tunnel Particle Image Velocimetry (PIV) measurements may be used to predict full-scale flow dynamics from the, typically, very limited number of field measurement sensors.

1. Introduction

Wind tunnels are frequently used to model urban street canyon turbulence and ventilation dynamics (Kastner-Klein and Rotach, 2004; Savory et al., 2013). However, there have been few cases in which the mean and unsteady flow dynamics from a wind tunnel and field study have been quantified and compared in order to justify the validity of the wind tunnel results. Much previous full-scale work has been completed to study the dispersion of pollutants in urban areas, such as the Mock Urban Setting Test (MUST) (Biltoft et al., 2002) and examination of the dispersion in existing urban areas in the Hamamatsu-cho Minato-ku area of Tokyo, Japan (Tominaga et al., 2013), Gottinger Strasse, Hanover and Jagtvej, Copenhagen (Ketzel et al., 2000). Other researchers have conducted significant flow measurements with the most common type being in-situ measurements within urban areas. These studies, such as the Oklahoma City Joint Urban 2003 (JU2003) (Hanna et al., 2007), typically conduct flow measurements near street level and at building roof level, while others, such as the Nantes'99 experiment (Kastner-Klein and Rotach, 2004), have conducted measurements both within and above the street canyon. The majority of these studies consider only field measurements. However, to better understand the wind flow dynamics of the urban environment and how to model them, one must consider comparable wind tunnel models. Studies including significant wind tunnel measurements include the Nantes'99 experiment (Kastner-Klein and Rotach, 2004), the Basel UrBan Boundary Layer Experiment (BUBBLE) (Rotach et al., 2005) and the Comprehensive Outdoor Scale MOdel (COSMO) (Takimoto et al., 2011). From the literature it may be seen that many studies have investigated the flow within urban areas using field data either in-situ, within a specific urban location, or within simplified roughness arrays set-up at a test site (COSMO). However, due to the complexity of the urban environment and the challenges of conducting studies within the atmospheric boundary layer such research has provided only limited information about the flow dynamics governing street canyon ventilation. From this review an important question still remains; does a properly scaled wind tunnel model reproduce the main flow features within a full-scale street canyon that govern ventilation?

2. Experimental details

This work consists of two phases of experimentation. The first is a field study, which will be discussed in the first section and the second is a wind tunnel study of equivalent reduced-scale geometry.

2.1 Field experiment

Field data were provided from the *Influence des effets micro-météorologiques sur la propagation acoustique en milieu urbain* (EM2PAU) campaign (Guillaume et al., 2012) which took place in Nantes, France, over a two-year period. Sonic anemometers with built-in thermocouples (S11 to S16: Gill WindMaster, S10, on the mast: Metek USA1-1 FSA) were used to measure the three components of velocity, as well as temperature, within an idealized canyon. The canyon was made from shipping crates, giving an aspect ratio of width to height, W/h =

0.70 and length to height, L/h = 4.62, and was located in a parking lot surrounded by woods and fields with some buildings nearby, outside of the city of Nantes. The present paper focuses on wind flows perpendicular to the canyon axis. These are winds coming from the 313^o and from the 133^o direction. From the north-west (approach flow from the 313^o direction) the terrain is wooded and will have a z_o of approximately 0.3 m (ESDU 1982; 1985) while from the south-east (approach flow from the 133^o direction) the terrain is flat grassland and fields resulting in a z_o range of 0.03 – 0.1 m (ESDU 1982; 1985). These correspond to displacement heights for the 133^o and 313^o approach flow directions of between 0-2 m and 5-7 m. Within the canyon there are six sonic anemometers aligned with the axis of the canyon all located 12.00 m from each of the canyon ends and spaced 0.80 m apart in the streamwise direction with three at a height of z/h = 0.38 (S14, S15, S16) and another three at z/h = 0.77 (S11, S12, S13) from the ground (Fig. 1a). A seventh sonic anemometer is located on a mast at 10.00 m height (S10), x/h = 1.66 and y/h = 4.94 away from the centre of the canyon, to determine the characteristics of the oncoming flow, and is aligned with the North direction (Fig. 1a). All of the sonic anemometers have an acquisition frequency of 20 Hz and measure *U*, *V*, *W* velocity components and temperature.

2.2 Wind tunnel experiment

The wind tunnel experiment was conducted in the low-speed, suck-down boundary layer wind tunnel in the Laboratoire de recherche en Hydrodynamique, Énergétique et Environnement Atmosphérique (LHEEA) at École Centrale de Nantes (Fig. 1b), which has working section dimensions of 2 m (width) x 2 m (height) x 24 m (length). The experiments used five 800 mm high vertical tapered spires located immediately downstream of the contraction and a 200 mm high solid fence across the working section 750 mm downstream of the spires to initiate the boundary layer development. Flow measurements were conducted using stereoscopic PIV at a frequency of 7 Hz to record all three components of velocity. 5000 pairs of images were recorded and the multi-pass cross-correlation PIV processing resulted in a final interrogation window size of 16 x 16 pixels with an overlap of 50%. The final spatial resolution was 0.83 mm and 1.68 mm in the longitudinal and vertical directions, respectively. The upstream roughness used in the current case consisted of 50 mm cubes arranged in a staggered array with λ_p = 25% and the canyon had an aspect ratio of W/h = 0.70 and L/h = 4.62 to match the field experiment. The wind tunnel boundary layer was scaled using ESDU and was found to best match a suburban terrain with z_o = 0.2 m and d = 0.045 m at a scale of 1:200 (ESDU 1982; 1985).

3. Results and discussion

3.1 Data selection and pre-processing

Data collection ran over the course of two years (2011-12) and was saved in continuous intervals of 15 minutes. Applicable periods of data for comparison with the wind tunnel experiment were extracted based on the following data selection criteria; flow direction was 133^o ± 15^o and 313^o ± 15^o, Monin-Obukhov length was a minimum of 1000 m to ensure neutral stability and these criteria had to be satisfied for a period of at least 30 minutes. After initial processing further criteria were applied. A test for stationarity was conducted (Lee et al., 2004) and to reduce the influence of the along-canyon wind any cases where the along-canyon wind was greater than 10% of the streamwise wind were removed. Using these criteria 12 periods and 5 periods were found for the 133^o and 313^o wind directions, respectively.

3.2 Mean turbulence statistics

The canyon statistics from the field data were compared to the profiles obtained from the wind tunnel PIV results. The mean velocities are normalized using the mean streamwise velocity measured at the mast and the turbulence intensities are normalized by friction velocity. Fig. 2 shows the streamwise, spanwise and vertical profiles along the centre axis of the canyon and is used as an example. There is consistency between the wind tunnel and field data for the streamwise velocity and turbulence intensity, which is generally within 20%. However, there is significant discrepancy in the spanwise statistics, which show for the spanwise velocity and spanwise turbulence intensity a difference of approximately 1000% and 100%, respectively. Significant spanwise velocity has been noted in several other studies in the literature (Arnfield and Mills, 1994). It has previously been attributed to the high-sensitivity of canyon flow to large-scale wind direction changes (Eliasson et al., 2006). In the current study the strong spanwise velocity could also be influenced by the changing wind direction, as exactly perpendicular and constant wind directions are not present in the atmospheric boundary layer.

3.3 Influence of ambient conditions on canyon statistics

In the present work the influence of the changing wind direction has been investigated by comparing the mean spanwise velocity and spanwise turbulence intensity for two cases, one with high and one with low standard deviation of the ambient wind direction. The two periods compared for each flow direction (Fig 3) had a normalized standard deviation of 7.8^o and 0.2^o for the 133^o approach flow direction and 8.6^o and 0.8^o for the 313^o approach flow direction. From Fig 3a it is evident that the lower standard deviation of the ambient wind direction results in better agreement, up to a factor of 6, in the mean spanwise velocity with the wind tunnel results for both approach flow directions. However, the results still show large discrepancy suggesting that large mean spanwise velocity is present even for cases where wind direction changes are small. The mean spanwise turbulence intensity results demonstrate that the low standard deviation cases result in good agreement, within 30%, with the wind tunnel results at all sonic locations (Fig 3b). It can, therefore, be concluded that large wind direction changes result in both an increase in mean spanwise velocity and turbulence intensity.

To further clarify the causes of the discrepancies between the wind tunnel and field canyon turbulence intensities, the turbulence spectra within the field canyon were examined. Fig 4 shows the spectra for the upstream sonic anemometers located at x/W = -0.22 as an example. The results show significant low-frequency, large-scale motion in the spanwise direction. Inagaki and Kanda (2008) computed the turbulence spectra for all three velocity components at a height of z/h = 2 over a 25% aligned cube array. Their results show an influence of low-frequency motion in both the streamwise and spanwise turbulence spectra, being more pronounced in the spanwise velocity, as in the present study. In conclusion, these results show that even with a short averaging period and stringent selection criteria there is still a low frequency influence in the spanwise direction.

3.4 Canyon flow dynamics

The size of the turbulent structures in the streamwise, spanwise and vertical directions can be assessed by two-point spatial correlations. The correlation was performed for each 30 minute time period that passed the post-processing selection criteria outlined in Section 3.1. For comparison purposes the two-point spatial correlation was calculated using the PIV wind tunnel data for three velocity components (*U, V* and *W*). An example of the equation used to calculate the two-point spatial correlation is shown in Equation 1 for the streamwise velocity.

$$R_{uu}(x_{ref}, z_{ref}, x, z) = \frac{u'(x_{ref}, z_{ref}')u'(x, z)}{\sqrt{u'^2(x_{ref}, z_{ref}')}\sqrt{u'^2(x, z)}} \quad (1)$$

The two-point spatial correlations were computed using the sonic anemometer S12, located at z/h = 0.77 and x/W = 0, as the reference point and the streamwise correlation results are shown here (Fig. 5). The correlation coefficient of the streamwise velocity component averaged over all 30 minute periods shows significantly good agreement, to within 30%, with the wind tunnel results. However, the correlation of the spanwise velocity (not shown here) is overestimated by up to 50% by the wind tunnel results at the upstream (x/W = -0.22) sonic anemometers. Dissimilarly, the correlation of the vertical velocity (not shown here) is generally underestimated at all sonic positions by between 15-55% in the wind tunnel results when compared with both field approach directions. This discrepancy is likely a result of the differences in sizes of structures within the atmospheric boundary layer and the boundary layer produced in the wind tunnel. As seen previously, the field results display large, low-frequency spanwise motion that is not present in the wind tunnel

3.5 Stochastic Estimation

The good agreement between the results obtained using the wind tunnel model and during the field experiment has been demonstrated in the previous sections. In particular, the good match, within 15-30%, between the two-point correlation coefficients shows that the wind tunnel model reproduces well the organization of the main turbulent structures. Based on that, the spatially well-resolved wind tunnel data combined with the Quadratic Stochastic Estimation (QSE) method are used here to spatially extrapolate the sparse data from the field experiment. This technique, first introduced by Adrian (1977) as a mathematical approximation of conditional averages in order to identify coherent structures in turbulent flows, is based on the knowledge of the two-point statistics of the flow up to the fourth order in the region where the velocity field is to be estimated and uses the simultaneous measurements of the velocity at a few selected reference positions. This approach allows the construction of a model for the time-evolution of the instantaneous flow in the plane containing the 6 sonic anemometers, which is based on the wind tunnel data and driven by the instantaneous reference velocity signals from the field experiment. In its quadratic version, the model is of the form:

$$\tilde{u}_i(x, y, z, t) = \sum_{j=1}^{N_c} \sum_{l=1}^{N_{ref}} A_{jl}^i u_j^{ref}(x_l, y_l, z_l, t) + \sum_{j,l=1}^{N_c} \sum_{m,n=1}^{N_{ref}} B_{jlmn}^i u_j^{ref}(x_m, y_m, z_m, t) u_k^{ref}(x_n, y_n, z_n, t) \quad (2)$$

where $\tilde{u}$ is the modeled velocity field from the knowledge of u^{ref} at N_{ref} locations (here the 6 sonics). For an extensive description, the reader is referred to the work of Adrian (1977) and Guezennec (1989).

In the present study QSE has been used to derive a model with velocity time-series from the sonic anemometers as reference signals to estimate the corresponding instantaneous velocity field in the entire canyon cross-section. The results presented here are based on a single 45 min period during which the ambient wind direction was from 133°. The database obtained consists of 54000 bi-dimensional, two-component vector fields with the same temporal frequency as the original field measurements (20 Hz). The mean velocity flow field obtained from the wind tunnel database, properly scaled by the ambient wind velocity, is used to reconstruct the complete velocity field. Examples of the instantaneous vector fields of the velocity fluctuations are presented in Fig 6. The QSE flow field shows the presence of large-scale motions consisting of intermittent ejections and penetrations of fluid across the canyon opening and recirculation of fluid within the canyon accompanied by smaller-scale vortices. The intermittent presence of the flapping shear layer developing from the upstream canyon obstacle is also well-reproduced. These flow features have already been observed in wind tunnel studies of street canyons with AR = 1 (Perret and Savory, 2013). The corresponding statistics, presented in Fig. 7, show good agreement with those obtained from the wind tunnel experiment. In particular, the high level of σ_u inside the shear-layer, the high level of σ_w along the vertical wall of the downstream building and the magnitude of the Reynolds shear stress at the canyon opening are well-reproduced.

4. Conclusion

The turbulence statistics from the simple street canyon model studied in the EM2PAU campaign (Guillaume et al., 2012), which took place in Nantes, France, and a wind tunnel model of equivalent geometry were investigated. The mean turbulence statistics were well predicted within the canyon by the wind tunnel model except in the case of the mean spanwise velocity and spanwise turbulence intensity. This discrepancy was found to be a result of the changing approach flow wind direction. As the wind shifts direction over time the effect is a channeling of flow along the canyon axis. The wind tunnel model, although of equivalent geometry, produces nominally 2D flow and, therefore, cannot accurately represent the spanwise flow phenomena of channeling. Finally, Quadratic Stochastic Estimation was used with the PIV and sonic anemometers to estimate the two-dimensional flow fields of the field experiment. The results from the QSE constitute, to the authors' knowledge, the first attempt to combine spatially well-resolved PIV data obtained from a wind tunnel experiment with time-resolved but sparse velocity measurements from a field experiment representing the same street canyon configuration. The use of Stochastic Estimation with combined data from wind tunnel and field experiments offers great potential for the prediction of the ventilation inside the street canyon and for the design of field experiments for which the optimum location of sensors can be studied beforehand, depending on the objectives of the particular study. Current knowledge of canyon flows from field studies is limited, as most previous work has been focused on dispersion (Biltoft et al., 2002; Tominaga et al., 2013; Ketzel et al., 2000). The present work is a significant contribution to the field of environmental fluid mechanics as it provides a detailed comparison with a wind tunnel model of equivalent geometry (Kastner-Klein and Rotach, 2004; Rotach et al., 2005; Takimoto et al., 2011) and detailed analysis of turbulence statistics within the canyon, both of which are not commonly done for canyon flow studies.

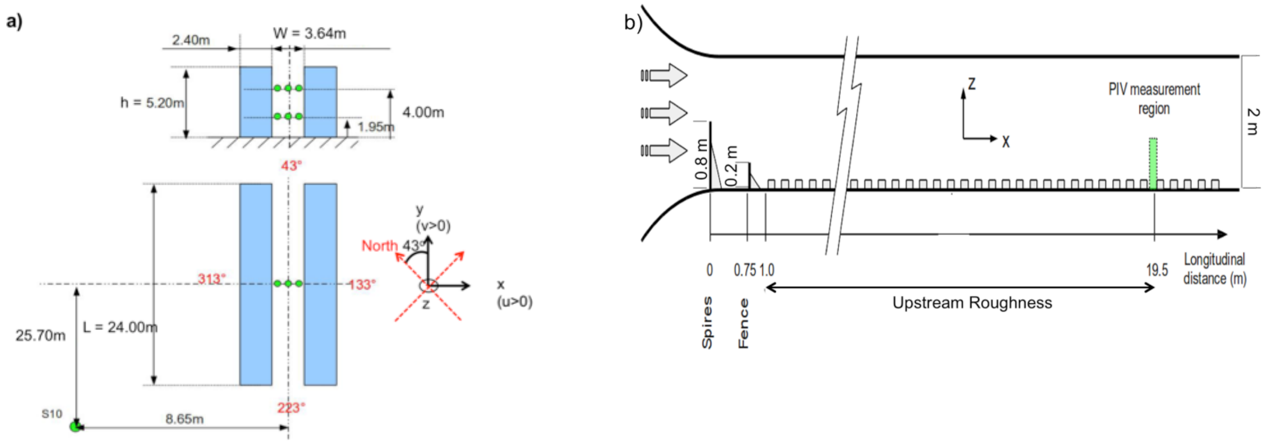

Fig. 1 a) Elevation and plan view of canyon and mast; b) Wind tunnel set-up.

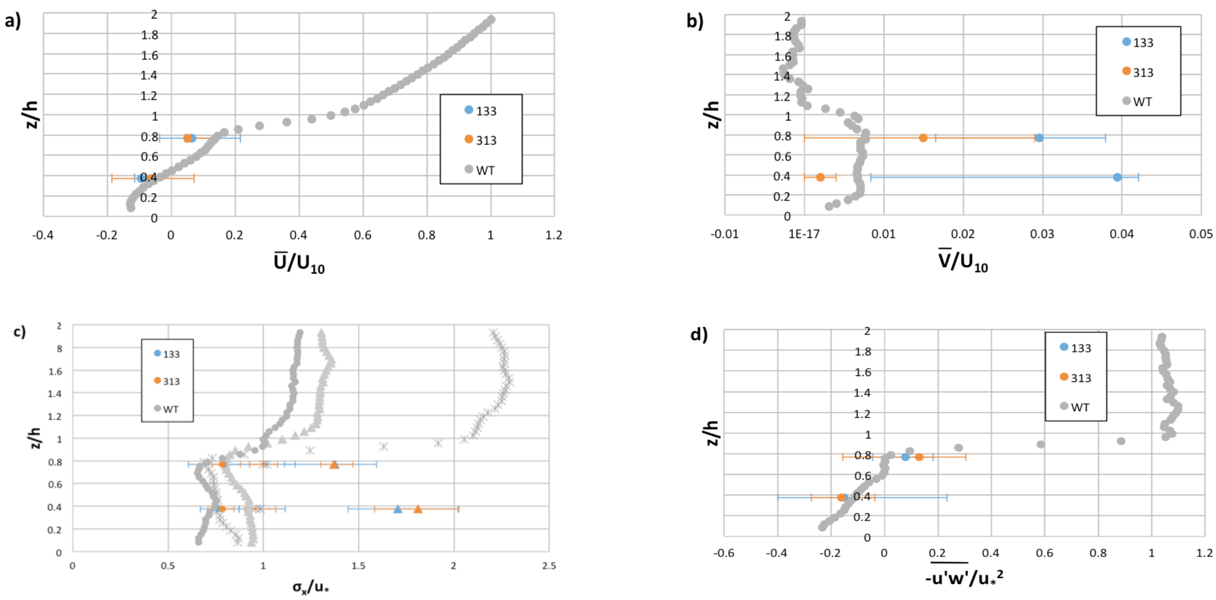

Fig. 2 Field data and wind tunnel PIV profiles at centre (y/h = 0) of canyon at x/W = 0 a) streamwise velocity; b) spanwise velocity; c) streamwise (x), spanwise (Δ) and vertical (•) turbulence intensity d) Reynolds shear stress.

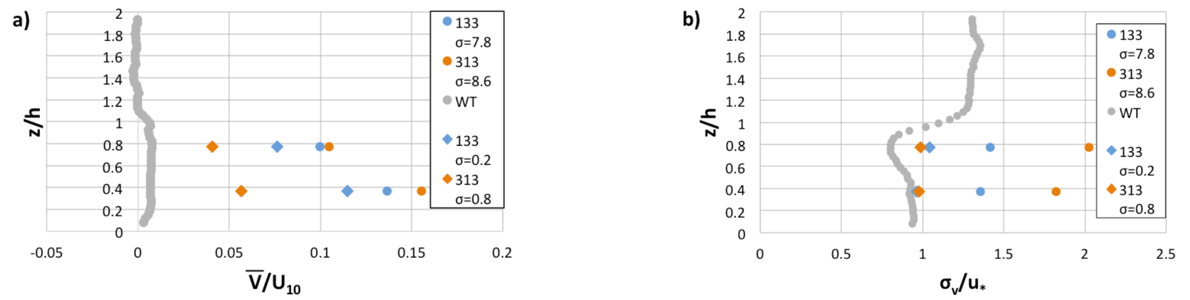

Fig. 3 Time averaged mean a) spanwise velocity; b) spanwise turbulence intensity at centre (y/h = 0), x/W = 0 of canyon compared with wind tunnel PIV results with high and low standard deviation (σ°) of ambient wind.

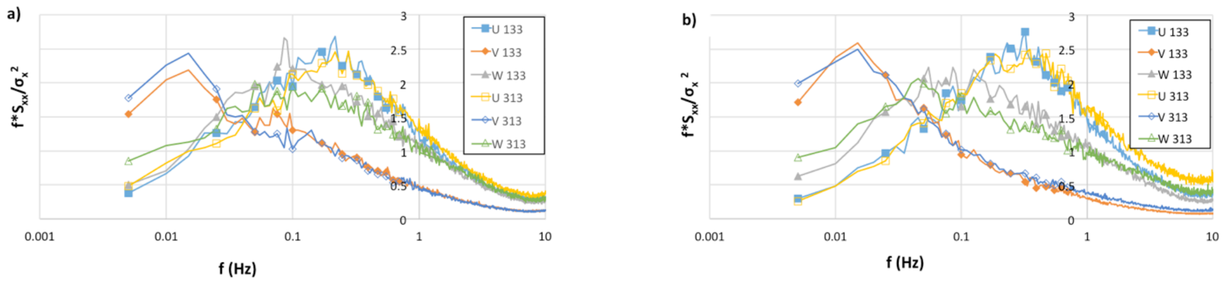

Fig. 4 Ensemble averaged turbulence spectra showing both ambient wind directions and all three turbulence components at the canyon centre (y/h = 0) at x/W = -0.22 and a) z/h = 0.38; b) z/h = 0.77. The symbols used here are to aid in interpretation when viewing in grey-scale and are not data points.

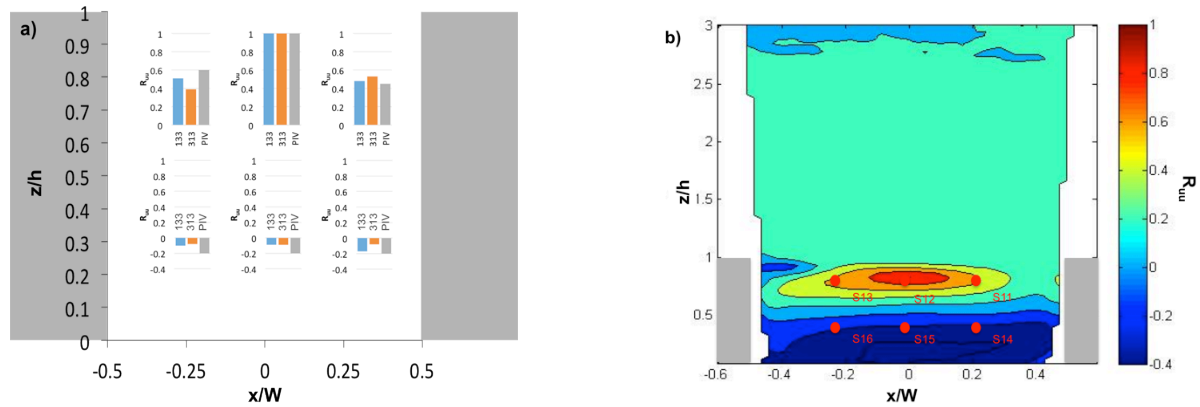

Fig. 5 a) Two-point spatial correlation coefficient magnitudes of sonic anemometers along with wind tunnel PIV with reference point (x_{ref}/W, z_{ref}/h) = (0, 0.77) for streamwise velocity component (u'); b) streamwise (u') velocity component two-point correlation of wind tunnel PIV with reference point (x_{ref}/W, z_{ref}/h) =(0, 0.77) showing field sonic anemometers (•).

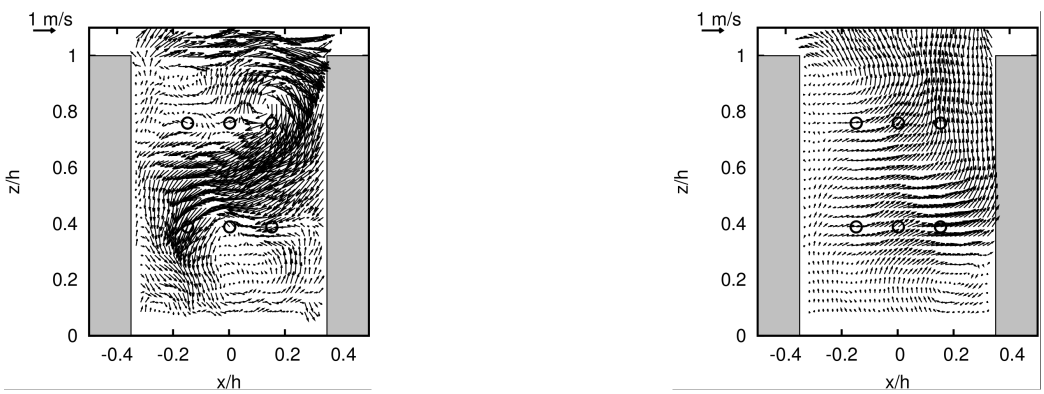

Fig. 6 Examples of two different instantaneous velocity fields obtained by QSE using the 6 simultaneous measurements by sonic anemometers from the field experiment (○) and the QSE coefficient determined from the wind tunnel experiment (only the fluctuations are shown).

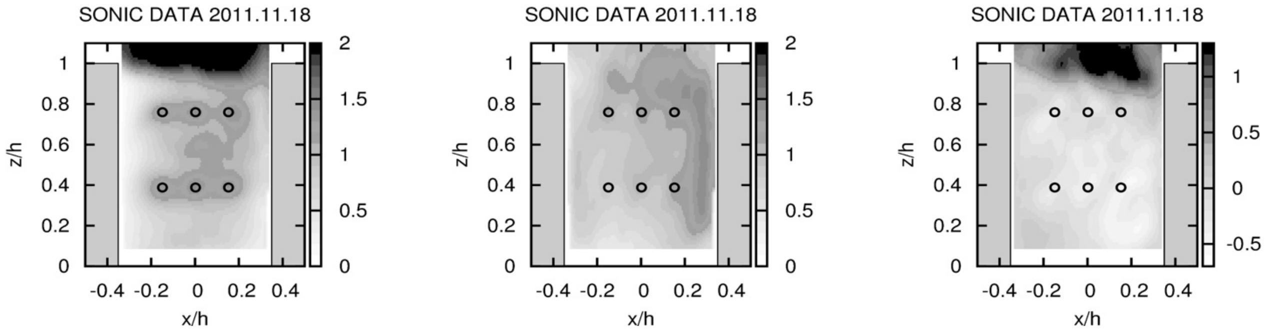

Fig. 7 Statistics, σ_u (left), σ_w (centre), u'w' (right), of the velocity field obtained by QSE using the 6 simultaneous measurements by sonic anemometers from the field experiment (○) and the QSE coefficient determined from the wind tunnel experiment.

References

Adrian, R.J., 1977. On the role of conditional averages in turbulence theory. In Turbulence in Liquids; Proc 4th *Biennial Symp on Turbulence*, Rolla, Mo., 22-24 Sep 1975, (Princeton, N.J: Science Press), 323-332.

Arnfield A.J., Mills G.M., 1994. An analysis of the circulation characteristics and energy budget of a dry, asymmetric, east-west urban canyon. I. Circulation characteristics. *Int J Climatol,* **14**, 119-134.

Biltoft C.A., Yee E., Jones C.D., 2002. Overview of the Mock Urban Setting Test. *Proc 4th Symp on the Urban Environment, Norfolk, Virginia, USA*.

Eliasson I., Offerle B., Grimmond C.S.B., Lindqvist S., 2006. Wind fields and turbulence statistics in an urban street canyon. *Atmos Environ,* **40**, 1-16.

ESDU, 1982. Strong winds in the atmospheric boundary layer. Part I: mean-hourly wind speeds. Data Item 82026 (amended 1993). *Engineering Sciences Data Unit International.*

ESDU, 1985. Characteristics of atmospheric boundary layer. Part II: single point data for strong winds (neutral atmosphere). Data Item 852020 (amended 1993). *Engineering Sciences Data Unit International.*

Guezennec, Y.G. , 1989. Stochastic estimation of coherent structures in turbulent boundary layers. *Phys Fluids A*, **1**, 1054-1060.

Guillaume G., Ayrault C., Berengier M., Calmet I., Gary V., Gaudin D., Gauvreau B., L'hermite Ph., Lihoreau B., Perret L., Picaut J., Piquet T., Rosant J.M., Sini J.F., 2012. Micrometeorological effects on urban sound propagation: a numerical and experimental study. *All Glo Sus*, **19**, 109-119.

Hanna S., White J., Zhou Y., 2007. Observed winds, turbulence and dispersion in built-up downtown areas of Oklahoma City and Manhattan. *Bound Layer Meteorol*, **125**, 441-468.

Inagaki A., Kanda, M., 2008. Turbulent flow similarity over an array of cubes in near-neutrally stratified atmospheric flow. *J Fluid Mech*, **615**, 101-120.

Kastner-Klein P., Rotach M.W., 2004. Mean flow and turbulence characteristics in an urban roughness sublayer. *Bound Layer Meteorol,* **111**, 55-84.

Ketzel M., Berowicz R., Lohmeyer A., 2000. Comparison of numerical street dispersion models with results from wind tunnel and field measurements. *Environ Monit Asses*, **65**, 363-370.

Lee X., Massman W.J., Law B., 2004. Handbook of micrometeorology: a guide for surface flux measurements and analysis. *Kluwer Academic Publishers, The Netherlands* pp. 181-208.

Liu H.Y., Bo T.L., Wang G.H., Zheng X.J.,2014. The analysis of turbulence intensity and Reynolds shear stress in wall-bounded turbulence flows at high Reynolds numbers. *Bound Layer Meteorol* **150**, 33-47.

Perret L., Savory E., 2013. Large-scale structures over a single street canyon immersed in an urban-type boundary layer. *Bound Layer Meteorol*, **148**, 111-113.

Rotach M.W., Vogt R., Bernhofer C., Batchvarova E., Christen A. et al., 2005. BUBBLE – an urban boundary layer meteorology project. *Theor Appl Climatol*, **81**, 231-261.

Savory E;, L. Perret L., Rivet C., 2013. Modelling considerations for examining the mean and unsteady flow in a simple urban-type street canyon. *Meteorol Atmos Phys,* **121**, 1-16.

Takimoto H., Sato A., Barlow J.F., Moriwaki R., Inagaki A., Onomura S., Kanda M., 2011. Particle image velocimetry measurements of turbulence flow within outdoor and indoor urban scale models and flushing motions in urban canopy layers. *Bound Layer Meteorol,* **140**, 295-314.

Tominaga Y., Iizuka S., mano M., Kataoka H., Mochida A., Nozu T., Ono Y., Shirasawa T., Tsuchiya N., Yoshie R., 2013. Cross comparisons of CFD results of wind and dispersion field for MUST experiment: evaluation exercises by AIJ. *J Asian Arch Build Eng,* **12**, 117-124.